

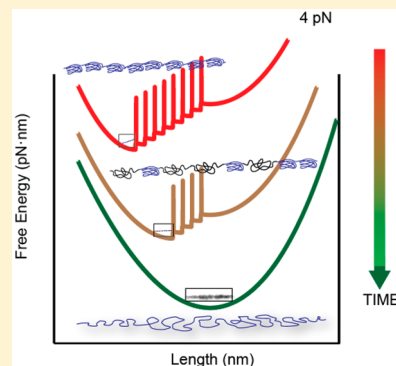
Proteins Breaking Bad: A Free Energy Perspective

Jessica Valle-Orero,^{*†} Rafael Tapia-Rojo, Edward C. Eckels, Jaime Andrés Rivas-Pardo, Ionel Popa,[†] and Julio M. Fernández

Department of Biological Sciences, Columbia University, New York, New York 10027, United States

Supporting Information

ABSTRACT: Protein aging may manifest as a mechanical disease that compromises tissue elasticity. As proved recently, while proteins respond to changes in force with an instantaneous elastic recoil followed by a folding contraction, aged proteins *break bad*, becoming unstructured polymers. Here, we explain this phenomenon in the context of a free energy model, predicting the changes in the folding landscape of proteins upon oxidative aging. Our findings validate that protein folding under force is constituted by two separable components, polymer properties and hydrophobic collapse, and demonstrate that the latter becomes irreversibly blocked by oxidative damage. We run Brownian dynamics simulations on the landscape of protein L octamer, reproducing all experimental observables, for a naive and damaged polyprotein. This work provides a unique tool to understand the evolving free energy landscape of elastic proteins upon physiological changes, opening new perspectives to predict age-related diseases in tissues.



The discovery that massively large tandem modular proteins play a crucial role in cellular functioning has shifted our view on the molecular origins and regulation of protein mechanics.^{1–6} For instance, the unfolding/refolding of the numerous domains of the giant protein titin contributes to the elasticity of the muscle, and assists muscle contraction.⁵ Similarly, the extracellular proteins involved in the adhesion of bacteria to their targets have a tandem configuration that allows them to withstand large mechanical drag forces from coughing or sneezing.⁶ These complex systems have the ability to extend to different lengths once unfolded, or inversely contract to their native state when force is reduced.^{7–10} The extensibility of elastic proteins is essential in biological processes such as tissue elasticity, cell–cell signaling, and bacteria adhesion among others.^{2,11}

However, it has been recently demonstrated how age-related deterioration of elastic polyproteins eventually compromises their mechanical properties.¹² Under normal conditions, a naive (unmodified) unfolded polyprotein contracts in two stages when the force is reduced: an instantaneous elastic recoil determined by its polymer properties, followed by a slower folding contraction driven by the hydrophobic collapse to the native state.^{13,14} Protein side chains, which become exposed during mechanical unfolding, are then modified by naturally occurring reactive oxygen species resulting in a gradual loss of protein folding. Protein oxidative damage, which *in vivo* becomes apparent only after decades of exposure, can be greatly accelerated using ultrastable magnetic tweezers instrumentation to keep proteins mechanically unfolded for very long periods of time. Upon reducing the force, the protein can no longer contract through folding, and the damage is irreversible. Cryptic oxidation is what causes proteins to “break bad” or lose their capability to fold, and it is a hallmark of

protein aging.^{15–18} The consequent reduction of the mechanical integrity of elastic polyproteins is associated with the loss of tissue elasticity.

When dealing with molecular systems at these scales, the language of free energy landscapes is a common one, since it provides deep physical insight and allows for a predictive capability under different external conditions.^{19–23} In particular, understanding the elastic properties of tandem modular proteins within this context supposes a highly nontrivial enterprise.^{24,25} A rigorous description on that level should convolute the folding properties of the domains with the nonhookean response of the polypeptide chain to force.^{26–28} Recently, we proposed a mesoscopic model for the free energy landscape of polyproteins under force, which integrates the hydrophobic collapse of the individual domains with the intrinsic polymer properties of the polypeptide chains.²⁹ However, the outcome of our model was never systematically contrasted with force spectroscopy experiments. Also, we never took advantage of its predictive capability to discuss how the elastic properties would be modified under different physiological conditions such as post-translational modifications or oxidative stress.

In this work, we aim to provide a full description on how the free energy landscape of a polyprotein evolves as it ages, until the hydrophobic collapse of individual domains is impeded. We characterize the elastic behavior of a naive (nonoxidized) protein L octamer.³⁰ Using magnetic tweezers force spectroscopy, we provide the kinetic, equilibrium, and polymer properties over the wide range of forces (4–100 pN), allowing

Received: June 14, 2017

Accepted: July 19, 2017

Published: July 19, 2017

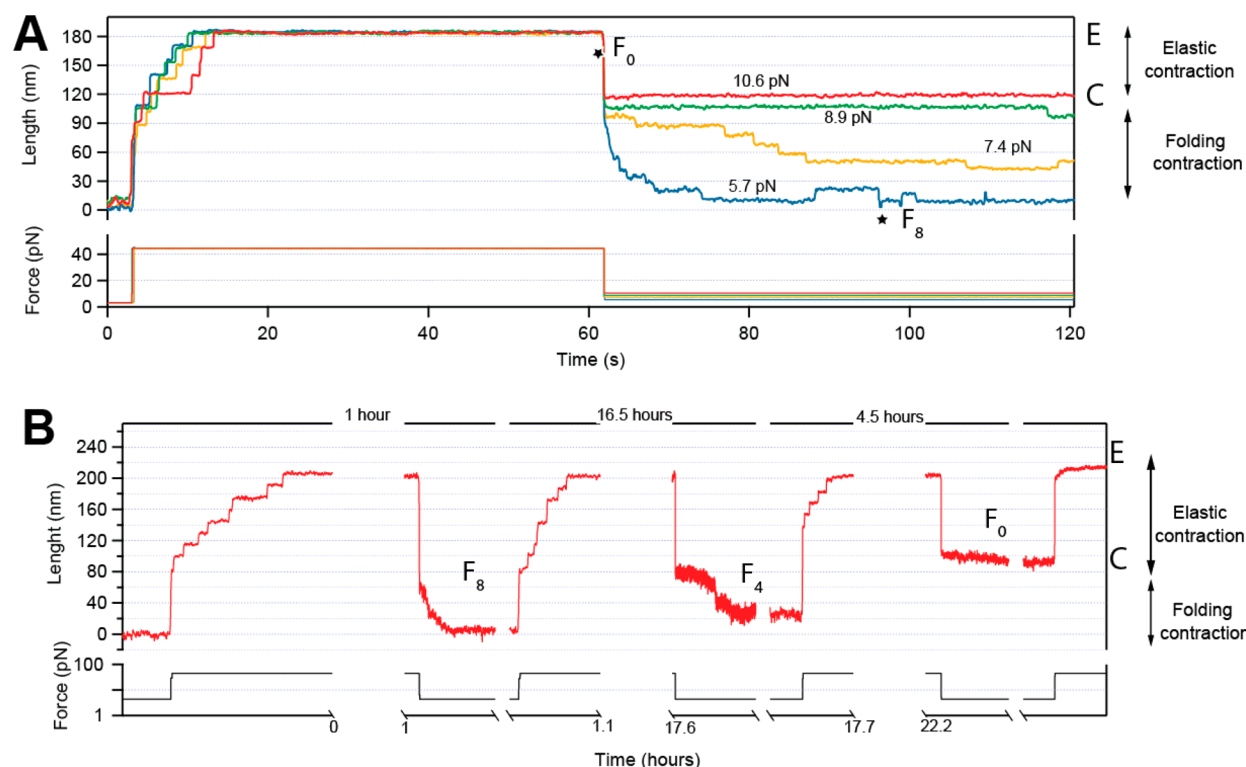


Figure 1. Magnetic tweezers measurements of protein L octamer under force. (A) Unfolded and extended protein L octamer (E) refolds at low forces (5.7 to 10.6 pN). Protein dynamics with complete refolding (<6 pN; F_8), coexistence of unfolded/folded states (6–9 pN), and complete unfolding (≥ 10 pN; C). (B) Experimental trace of protein L octamer during domain oxidation. In the last period of the trace all domains were damaged by oxidation and could not fold, becoming a random coil (F_0). The elastic recoil that a protein undergoes during refolding is composed of two elements: elastic contraction (E–C), and a folding contraction (C– $F_8/F_4/F_0$).

for a full description of the response of the polyprotein upon force changes.³¹ One of the keystones of our free energy landscape is how the folding of each domain and the elastic response of the polypeptide chain constitute two separable components, which are independently added to construct the free energy landscape of the polyprotein. This central hypothesis is corroborated when modeling the aging landscape. The components representing the hydrophobic collapse of each domain are removed, while the polymer behavior is kept unchanged. We use Brownian dynamics simulations on our model to reproduce accurate experimental benchmarks for a naive polyprotein, and compare them to those measured for a damaged polyprotein. Our work validates that the hydrophobic collapse is the driving component of folding contraction and, combined with the polymer response of the polypeptide, determines protein folding under force.

Figure 1A shows magnetic tweezers (MT) traces demonstrating the refolding dynamics of an unfolded protein L octamer (Figure S1A) when the force is reduced between 10–6 pN. Quenching to forces lower than 10 pN results in the instantaneous collapse of the extended chain (elastic contraction), followed by a slower folding contraction due to the folding of individual domains. These two distinguishable features correspond to the two main components of protein folding under force: hydrophobic collapse and polymer elasticity. The latter can be simply described as the entropic collapse of the unfolded polypeptide chain; by contrast, the folding contraction has a much more complex nature and occurs just at low forces, when the domains collapse toward the native state. Within this range of forces (4–10 pN) each protein L domain has a nonzero probability to visit the folded

and unfolded state. These folding transitions are highly sensitive to force, and provide enough information to measure the probability of folding and the distance at which the polypeptide equilibrates at each force.

The folding contraction can be compromised by the effects of reactive oxygen species which are generally present in physiological environments. Figure 1B shows a trace where the eight protein L domains are subjected to an unfolding force for long periods of time, throughout which the cryptic side chains that were buried in the native structure are exposed to reactive oxygen species.¹² The accumulation of oxidative modifications on these cryptic side chains can introduce unfavorable modifications that might eventually prevent the folding pathway, and thus lead to an overall reduction of the folding contraction (from F_8 to F_4 , until folding is completely blocked in F_0). Interestingly, such domain loss occurs in an all-or-none fashion and, unlike other oxidative modifications,³² is irreversible.

A complete characterization of the free energy landscape of the protein L octamer under force requires a correct description of the set of three mechanoelastic properties: the elastic contraction, the unfolding kinetics, and the equilibrium dynamics. We parametrize our free energy model by contrasting it with magnetic tweezers force spectroscopy data over a large force regime (4–100 pN). For the first time we validate our proposed model with experimental data, and furthermore provide an explanation of the effects of oxidative aging into the free energy landscape of polyproteins under force.

We use a freely jointed chain (FJC) model to describe the elastic properties of the polypeptide chain, and a Morse

potential with a Gaussian entropic barrier to model the hydrophobic collapse or folding transition.^{29,33} One of the main advantages of the model is that it can be parametrized by accounting independently for each of the three mentioned mechanoelastic properties, which are characterized by the mechanical observables from force spectroscopy experiments. First, the elastic response of the protein during unfolding/refolding is determined by the step-size length Δx_{NU} , following common polymer models such as the FJC.^{5,27} The equilibrium properties of the elastic polypeptide are associated with the Morse potential. Therefore, the folding probability can be used to determine the depth of the Morse well U_{M0} (see Supporting Information (SI)). Finally, the kinetic behavior of the polypeptide, in particular the unfolding kinetics, is dominated by the combination of the Morse potential and the Gaussian entropic barrier. However, once the depth U_{M0} is defined, the unfolding kinetics are independently determined by the parameters of the entropic barrier, the height U_{G0} , the width σ , and the distance to the transition state x^\ddagger (Figure 2). All these three parameters can be tuned by measuring the unfolding rates of the polypeptide.

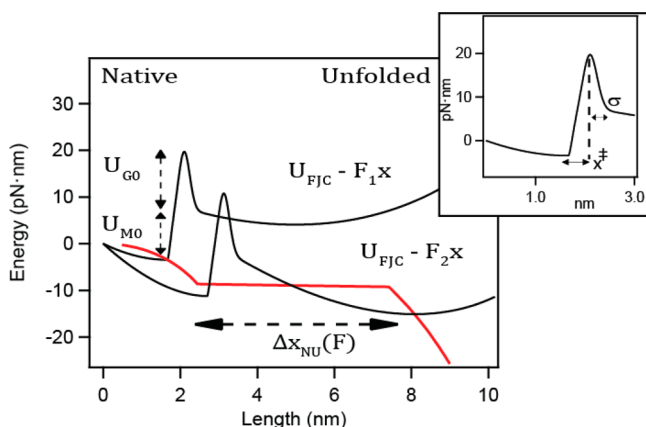


Figure 2. Scheme of the elements composing the free energy model of a protein of one domain under force. The native state is described by a Morse well of U_{M0} depth and a Gaussian barrier of U_{G0} height, both separated by a distance x^\ddagger (inset). The unfolded state is defined by the FJC model $U_{\text{FJC}} - Fx$, and shows how the distance between minima Δx_{NU} increases with force. The red curve tracks the global minimum of the profile as a function of force. At a pulling force of F_1 the unfolded state is at a higher energy than the folded state, thus becoming the most favored state. At a higher pulling force F_2 , the global minimum is shifted to coincide with the unfolded state.

The average size of the unfolding/refolding steps as a function of the pulling force is described with a FJC model with contour length increment of $\Delta L_c = 16.3$ nm and Kuhn length $l_k = 1.1$ nm (Figure 3A; solid line). From the equilibrium trajectories at constant force we measured the probability of folding, the time-averaged number of domains (red squares), and the most likely folding state (blue circles). This quantity can be readily accessed from our model by tracking the position of the global minimum in the free energy profile (red line Figure 2 and S1B) as a function of the force, and normalized by the total number of domains (black line Figure 3B, see SI). The theoretical force-dependent global minimum, obtained for $U_{\text{M0}} = 1.8$ kT, shows excellent agreement with the experimental data. Remarkably, the folding probability spans from 1 to 0 in a narrow force regime (4–10 pN),⁵ a consequence of the

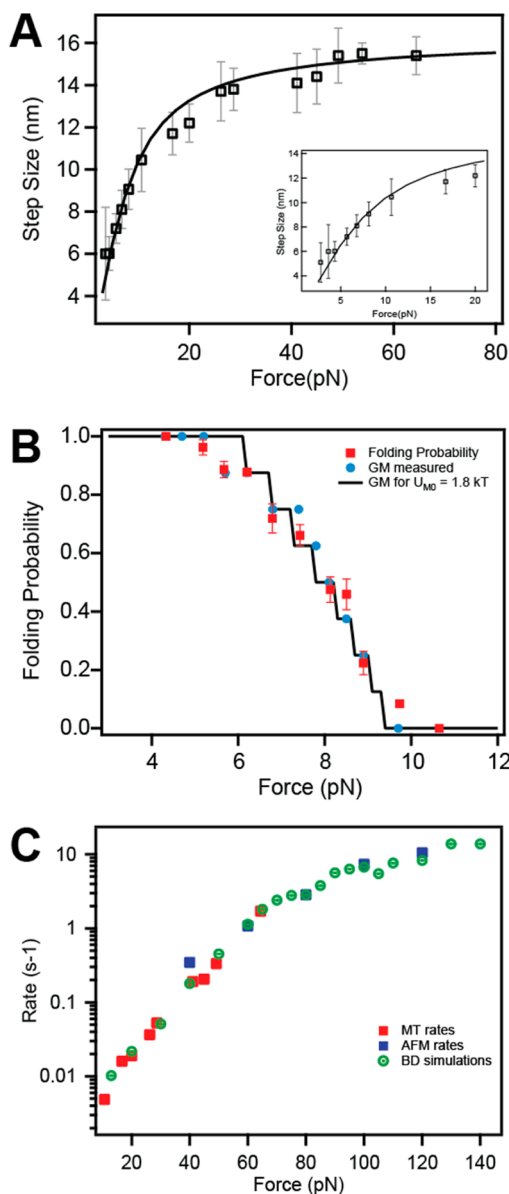


Figure 3. (A) The average step size of unfolding and folding traces as a function of force, fit with the FJC model of $l_k = 1.1$ nm and $\Delta L_c = 16.3$ nm. Error bars represent standard deviation. The insert is a zoom of the low-force regime. (B) Measurements of the probability of folding (red) and the most likely state (global minimum, GM; blue) as a function of refolding force obtained from traces similar to those in Figure 1A. The free-energy model with a Morse potential of $U_{\text{M0}} = 1.8$ kT provides the force dependency of the global minimum (most likely state) that fits the experimental data (solid black line). (C) Unfolding rates versus force from unfolding traces at a pulling force (13–120 pN) using AFM (blue symbols), and MT (red symbols). Brownian dynamics (BD) simulations of unfolding traces were run on our free-energy model (green curve) with $U_{\text{G0}} = 12$ kT, $\sigma = 0.025$ nm, and $x^\ddagger = 0.44$ nm. Error bars represent standard errors of the mean.

nonlinearity of the polymer elasticity. Unfolding kinetics can be sufficiently described with first-order kinetics, since the transition state barrier is very short (only a few angstroms) for most proteins due to cooperativity effects. We calculate the unfolding rates by averaging measured traces for each force and fitting a single exponential.³⁴ Figure 3C shows a compilation of the unfolding rates measured with both magnetic tweezers (MT; red symbols) and atomic force microscopy (AFM; blue

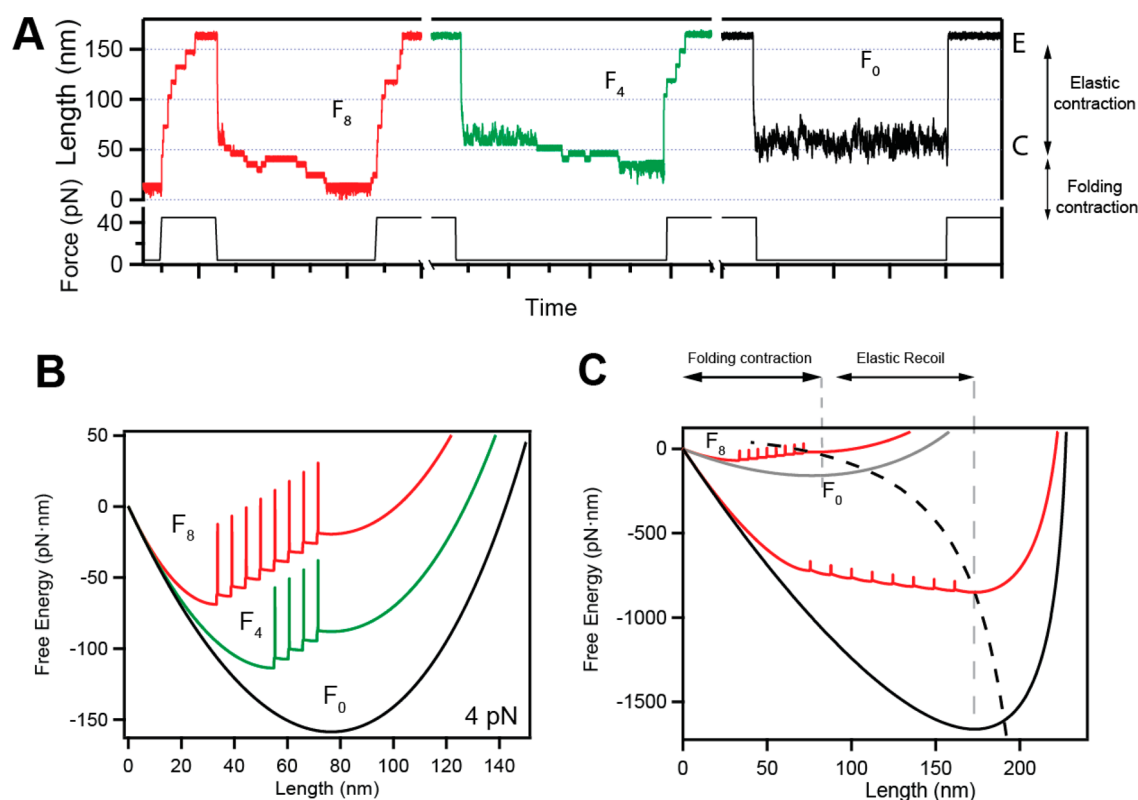


Figure 4. Protein oxidation causes the loss of protein folding. (A) Brownian dynamic simulation on the free energy model of eight tandem domains of protein L during domain oxidation. The trajectory simulates the unfolding of eight domains of protein L at 45 pN and then refolded at 4 pN, and how domain loss affects folding contraction. The loss of domains reduces the folding contraction when the force is reduced to 4 pN from F8 to F4, and finally F0, while shifting the global minimum of the free energy landscape as shown in panel B. The total loss of domains (black) can be simply reproduced with the FJC, $U_{\text{FJC}} = -Fx$. (C) Overview of the free energy landscape of a naive and damaged polyprotein under force. A fully unfolded and extended polyprotein of eight tandem domains is quenched to a low force (4 pN), rapidly collapses by the elastic recoil (following broken line), and subsequently undergoes refolding of the eight domains (F8). When the protein is oxidized during unfolding (black curve), the subsequent quench of the force results in the elastic recoil of the polymer to the low force free energy landscape (gray curve), in which the folding contraction is no longer available (F0).

symbols) techniques over a broad range of forces. We use Brownian dynamics simulations on our free energy model to generate unfolding trajectories (Figure S2). Matching the experimental and simulated unfolding rates, we determine the parameters of the entropic barrier that needs to be surmounted for the protein to unfold (responsible for the kinetic behavior of the system) as $U_{\text{G0}} = 12$ kT, $\sigma = 0.025$ nm, and $x^{\ddagger} = 0.44$ nm. Simulations on the free energy model reproduce the whole range of data, with diffusion constant of $D = 1500$ nm²/s (Figure 3C, green symbols). This is in agreement with previously reported values for AFM measurements in polyproteins³⁵ (see SI). Although this value might be different depending on the experimental probe, it will only alter the kinetics, and thus U_{G0} .

Our theoretical approach describes the total recoil under force as a combination of the hydrophobic collapse ($U_{\text{M}} + U_{\text{G}}$) and the elastic behavior ($U_{\text{FJC}} = -Fx$). Hence, owing to the ability of our model to capture the two distinguishable events observed experimentally, elastic recoil and folding contraction, Figure 4A reproduces the experimental results using Brownian dynamics on a free energy model that changes as domains oxidize (age). During domain-loss, neither the total extension of the unfolded protein (E) nor the polymer collapse due to elastic recoil during refolding (C) are affected by oxidation. However, the reduction of the folding contraction can be explained in our model by eliminating, domain-by-domain, the

components that drive protein folding ($U_{\text{M0}} = 0$ and $U_{\text{G0}} = 0$), and having the FJC energy, $U_{\text{FJC}} = -Fx$, as the sole term of the free energy profile of a domain. Figure 4B shows the free energy profile at 4 pN for 8 (red), 4 (green) and 0 (black) domains left. The loss of four domains, in the second pulse (green), leads to a shift of the global minimum to a higher length, which is represented experimentally and in the simulation by the loss in contraction between F8 and F4. Finally, the oxidation of all domains (black) is described by the FJC energy with a contour length of the whole polypeptide ($8 \cdot \Delta L_{\text{c}}$, where 8 is the total number of domains). Folding becomes fully inaccessible, and the global minimum is shifted to the fully unfolded state. Interestingly, our model shows that under a pulling force, the Morse potential can shift the equilibrium distance established by the FJC model (as in F0) to a lower length (F4 and F8), increasing the probability of folding over unfolding.

In this work, we have provided a full description of the free energy landscape of a tandem modular protein under force and, based on the foundations of the model, have predicted how this landscape evolves due to oxidative aging. From a more global perspective, the observations described here provide significant evidence for an element often dismissed when discussing protein folding under force: the polymer properties of the polypeptide chain. As we have shown, the end-to-end distance of the unfolded protein scales with force following polymer

models such as the FJC, which is inherently nonlinear, and acquires over half of its maximum extension below 10 pN, just in the range where proteins fold.³³ This fact is surprisingly dodged in most descriptions on protein folding/unfolding under force, starting with the fact that force is often modeled as an effective tilt in the landscape with a $-F \cdot x$ term.^{36–39} Conventional theoretical frameworks, such as the Bell–Evans model, are often used as a standard tool to describe the folding and unfolding kinetics of proteins under force.^{38,40} This approach might work in practice for describing protein unfolding kinetics, since Δx^\ddagger is typically very short (\sim angstroms). More recent extensions of the Bell–Evans model^{39,41,42} account for a shift of the transition state barrier due to the nonlinearity of the potentials that explains the curvature often observed at higher forces (Figure 3C). However, these approaches fail to provide an accurate description of the folding kinetics, where the transition states scales with force nonlinearly.

The combined Morse well and Gaussian barrier in our model represent a significant energetic barrier that needs to be overcome in order to reach the folded state. When the force is reduced and the polypeptide contracts considerably (elastic recoil), the hydrophobic amino acids push the water away, allowing their reorganization into a more confined state of lower conformational entropy. During protein oxidative damage, the irreversible modifications of the side-chains cause the loss of folding of the domains in an all-or-none matter. Our model can reproduce this behavior by removing the native components of each of the damaged domain. If oxidative modifications had been interpreted by changing the magnitudes of the Morse well and Gaussian barrier, the simulations would have shown deviations in the folding probability and kinetics, which were never observed experimentally. On the contrary, for instance, the loss of four domains does not show changes in the folding probability of the system at that force, (with still 100% at 4 pN). Additionally, the polymer character of the polypeptide chain together with protein hydrophobic collapse modulate the folding properties of polyproteins under force, since the landscape is tilted with nonlinear dependence ($U_{\text{FJC}} - F \cdot x$). Interestingly, most proteins fail to fold above 10 pN, and exhibit an abrupt decrease in the folding probability in a range of few piconewton, in general from 6–10 pN.^{2,5,33,43,44} Our model is able to capture this behavior, via the force dependency of the global minimum, whose force sensitivity is well understood considering the steepness induced by the Morse potential and the nonlinearity of the FJC model. These effects are more evident in proteins with a tandem modular arrangement, due to the high number of folding states. Most proteins with mechanical function in the physiological context show this tandem configuration,^{45–47} making our model relevant for capturing force-induced dynamics. Thus, understanding how polyproteins respond to force stimuli establishes how tissue elasticity, whether in the muscle, brain or skin, can be tuned under different physiological conditions.

The experimental and theoretical advances established in this work provide a novel view of the free energy of polyproteins under force, now permitting a more realistic modeling of tissue elasticity. Our model now allows simulating the changes in the mechanoelastic properties of a polyprotein as it ages, thus shedding some light on antiaging and elasticity regulating mechanisms of tissues. Hence, it could be used as a platform for evaluating phenotypes associated with diseases caused, for

instance, by post-translational modifications or mutations that will alter the mechanoelastic properties of the proteins.

■ ASSOCIATED CONTENT

Supporting Information

The Supporting Information is available free of charge on the ACS Publications website at DOI: 10.1021/acs.jpcllett.7b01509.

Detailed description of the force spectroscopy experimental methods, protein engineering materials, and summary of the physical concepts of the free-energy model and Brownian dynamics simulations (PDF)

■ AUTHOR INFORMATION

Corresponding Author

*E-mail: j.valleorero@gmail.com.

ORCID

Jessica Valle-Orero: 0000-0002-7010-1734

Present Address

[†]Department of Physics, University of Wisconsin-Milwaukee, WI 53211, United States

Notes

The authors declare no competing financial interest.

■ ACKNOWLEDGMENTS

This work was supported by the NSF Grant DBI-1252857, and by NIH Grants GM116122 and HL061228. R.T.R. was supported by Fundación Ramón Areces and ECE by the NHLBI (1F30HL129662). We would like to acknowledge Prof. Sergi Garcia-Manyes from King's College for his contribution with the unfolding AFM rates, and Jaykar Nayeck for his help in the development of the parallelism optimization of the BD simulations. Thanks to the members of the Fernandez lab for their fruitful discussions.

■ REFERENCES

- (1) Linke, W. A.; Hamdani, N. Gigantic business: titin properties and function through thick and thin. *Circ. Res.* **2014**, *114* (6), 1052–68.
- (2) del Rio, A.; Perez-Jimenez, R.; Liu, R. C.; Roca-Cusachs, P.; Fernandez, J. M.; Sheetz, M. P. Stretching Single Talin Rod Molecules Activates Vinculin Binding. *Science* **2009**, *323* (5914), 638–641.
- (3) Schoen, I.; Pruitt, B. L.; Vogel, V. The Yin-Yang of Rigidity Sensing: How Forces and Mechanical Properties Regulate the Cellular Response to Materials. *Annu. Rev. Mater. Res.* **2013**, *43*, 589–618.
- (4) Johnson, C. P.; Tang, H. Y.; Carag, C.; Speicher, D. W.; Discher, D. E. Forced unfolding of proteins within cells. *Science* **2007**, *317* (5838), 663–666.
- (5) Rivas-Pardo, J. A.; Eckels, E. C.; Popa, I.; Kosuri, P.; Linke, W. A.; Fernandez, J. M. Work Done by Titin Protein Folding Assists Muscle Contraction. *Cell Rep.* **2016**, *14* (6), 1339–1347.
- (6) Echelman, D. J.; Alegre-Cebollada, J.; Badilla, C. L.; Chang, C.; Ton-That, H.; Fernandez, J. M. CnaA domains in bacterial pili are efficient dissipaters of large mechanical shocks. *Proc. Natl. Acad. Sci. U. S. A.* **2016**, *113* (9), 2490–5.
- (7) Rief, M.; Gautel, M.; Oesterhelt, F.; Fernandez, J. M.; Gaub, H. E. Reversible unfolding of individual titin immunoglobulin domains by AFM. *Science* **1997**, *276* (5315), 1109–12.
- (8) Tskhovrebova, L.; Trinick, J.; Sleep, J. A.; Simmons, R. M. Elasticity and unfolding of single molecules of the giant muscle protein titin. *Nature* **1997**, *387* (6630), 308–12.
- (9) Yao, M.; Qiu, W.; Liu, R.; Efremov, A. K.; Cong, P.; Seddiki, R.; Payre, M.; Lim, C. T.; Ladoux, B.; Mege, R. M.; Yan, J. Force-dependent conformational switch of alpha-catenin controls vinculin binding. *Nat. Commun.* **2014**, *5*, 4525.

- (10) Yao, M.; Goult, B. T.; Klapholz, B.; Hu, X.; Toseland, C. P.; Guo, Y.; Cong, P.; Sheetz, M. P.; Yan, J. The mechanical response of talin. *Nat. Commun.* **2016**, *7*, 11966.
- (11) Miller, E.; Garcia, T.; Hultgren, S.; Oberhauser, A. F. The mechanical properties of *E. coli* type 1 pili measured by atomic force microscopy techniques. *Biophys. J.* **2006**, *91* (10), 3848–56.
- (12) Valle-Orero, J.; Rivas-Pardo, J. A.; Tapia-Rojo, R.; Popa, I.; Echelman, D. J.; Haldar, S.; Fernandez, J. M. Mechanical Deformation Accelerates Protein Ageing. *Angew. Chem.* **2017**, DOI: 10.1002/ange.201703630.
- (13) Bustamante, C.; Chemla, Y. R.; Forde, N. R.; Izhaky, D. Mechanical processes in biochemistry. *Annu. Rev. Biochem.* **2004**, *73*, 705–48.
- (14) Garcia-Manyes, S.; Dougan, L.; Badilla, C. L.; Brujic, J.; Fernandez, J. M. Direct observation of an ensemble of stable collapsed states in the mechanical folding of ubiquitin. *Proc. Natl. Acad. Sci. U. S. A.* **2009**, *106* (26), 10534–9.
- (15) Stadtman, E. R. Protein oxidation and aging. *Science* **1992**, *257* (5074), 1220–4.
- (16) Nystrom, T. Role of oxidative carbonylation in protein quality control and senescence. *EMBO J.* **2005**, *24* (7), 1311–7.
- (17) Stadtman, E. R. Protein oxidation and aging. *Free Radical Res.* **2006**, *40* (12), 1250–8.
- (18) Gorisse, L.; Pietrement, C.; Vuiblet, V.; Schmelzer, C. E.; Kohler, M.; Duca, L.; Debelle, L.; Fornes, P.; Jaisson, S.; Gillery, P. Protein carbamylation is a hallmark of aging. *Proc. Natl. Acad. Sci. U. S. A.* **2016**, *113* (5), 1191–6.
- (19) Stigler, J.; Ziegler, F.; Gieseke, A.; Gebhardt, J. C. M.; Rief, M. The Complex Folding Network of Single Calmodulin Molecules. *Science* **2011**, *334* (6055), 512–516.
- (20) Pierse, C. A.; Dudko, O. K. Distinguishing Signatures of Multipathway Conformational Transitions. *Phys. Rev. Lett.* **2017**, *118* (8), 088101.
- (21) Heidarsson, P. O.; Otazo, M. R.; Bellucci, L.; Mossa, A.; Imperato, A.; Paci, E.; Corni, S.; Di Felice, R.; Kragelund, B. B.; Cecconi, C. Single-molecule folding mechanism of an EF-hand neuronal calcium sensor. *Structure* **2013**, *21* (10), 1812–21.
- (22) Ritort, F. Single-molecule experiments in biological physics: methods and applications. *J. Phys.: Condens. Matter* **2006**, *18* (32), R531–83.
- (23) de Sancho, D.; Best, R. B. Reconciling Intermediates in Mechanical Unfolding Experiments with Two-State Protein Folding in Bulk. *J. Phys. Chem. Lett.* **2016**, *7* (19), 3798–3803.
- (24) Neupane, K.; Manuel, A. P.; Woodside, M. T. Protein folding trajectories can be described quantitatively by one-dimensional diffusion over measured energy landscapes. *Nat. Phys.* **2016**, *12* (7), 700.
- (25) Yuan, G.; Le, S.; Yao, M.; Qian, H.; Zhou, X.; Yan, J.; Chen, H. Elasticity of the Transition State Leading to an Unexpected Mechanical Stabilization of Titin Immunoglobulin Domains. *Angew. Chem., Int. Ed.* **2017**, *56* (20), 5490–5493.
- (26) Lannon, H.; Haghighanah, J. S.; Montclare, J. K.; Vanden-Eijnden, E.; Brujic, J. Force-clamp experiments reveal the free-energy profile and diffusion coefficient of the collapse of protein molecules. *Phys. Rev. Lett.* **2013**, *110* (12), 128301.
- (27) Berkovich, R.; Garcia-Manyes, S.; Klafner, J.; Urbakh, M.; Fernandez, J. M. Hopping around an entropic barrier created by force. *Biochem. Biophys. Res. Commun.* **2010**, *403* (1), 133–137.
- (28) Walther, K. A.; Grater, F.; Dougan, L.; Badilla, C. L.; Berne, B. J.; Fernandez, J. M. Signatures of hydrophobic collapse in extended proteins captured with force spectroscopy. *Proc. Natl. Acad. Sci. U. S. A.* **2007**, *104* (19), 7916–21.
- (29) Valle-Orero, J.; Eckels, E. C.; Stirnemann, G.; Popa, I.; Berkovich, R.; Fernandez, J. M. The elastic free energy of a tandem modular protein under force. *Biochem. Biophys. Res. Commun.* **2015**, *460* (2), 434–438.
- (30) O'Neill, J. W.; Kim, D. E.; Baker, D.; Zhang, K. Y. J. Structures of the B1 domain of protein L from *Peptostreptococcus magnus* with a tyrosine to tryptophan substitution. *Acta Crystallogr., Sect. D: Biol. Crystallogr.* **2001**, *57*, 480–487.
- (31) Popa, I.; Rivas-Pardo, J. A.; Eckels, E. C.; Echelman, D. J.; Badilla, C. L.; Valle-Orero, J.; Fernandez, J. M. A HaloTag Anchored Ruler for Week-Long Studies of Protein Dynamics. *J. Am. Chem. Soc.* **2016**, *138* (33), 10546–53.
- (32) Alegre-Cebollada, J.; Kosuri, P.; Giganti, D.; Eckels, E.; Rivas-Pardo, J. A.; Hamdani, N.; Warren, C. M.; Solaro, R. J.; Linke, W. A.; Fernandez, J. M. S-glutathionylation of cryptic cysteines enhances titin elasticity by blocking protein folding. *Cell* **2014**, *156* (6), 1235–46.
- (33) Valle-Orero, J.; Rivas-Pardo, J. A.; Popa, I. Multidomain proteins under force. *Nanotechnology* **2017**, *28* (17), 174003.
- (34) Popa, I.; Kosuri, P.; Alegre-Cebollada, J.; Garcia-Manyes, S.; Fernandez, J. M. Force dependency of biochemical reactions measured by single-molecule force-clamp spectroscopy. *Nat. Protoc.* **2013**, *8* (7), 1261–1276.
- (35) Berkovich, R.; Hermans, R. I.; Popa, I.; Stirnemann, G.; Garcia-Manyes, S.; Berne, B. J.; Fernandez, J. M. Rate limit of protein elastic response is tether dependent. *Proc. Natl. Acad. Sci. U. S. A.* **2012**, *109* (36), 14416–14421.
- (36) Guinn, E. J.; Jagannathan, B.; Marqusee, S. Single-molecule chemo-mechanical unfolding reveals multiple transition state barriers in a small single-domain protein. *Nat. Commun.* **2015**, *6*, 6861.
- (37) Jagannathan, B.; Marqusee, S. Protein folding and unfolding under force. *Biopolymers* **2013**, *99* (11), 860–9.
- (38) Alemany, A.; Rey-Serra, B.; Frutos, S.; Cecconi, C.; Ritort, F. Mechanical Folding and Unfolding of Protein Barnase at the Single-Molecule Level. *Biophys. J.* **2016**, *110* (1), 63–74.
- (39) Dudko, O. K.; Hummer, G.; Szabo, A. Intrinsic rates and activation free energies from single-molecule pulling experiments. *Phys. Rev. Lett.* **2006**, *96* (10), 108101.
- (40) Bell, G. I. Models for the specific adhesion of cells to cells. *Science* **1978**, *200* (4342), 618–27.
- (41) Friddle, R. W. Unified model of dynamic forced barrier crossing in single molecules. *Phys. Rev. Lett.* **2008**, *100* (13), 138302.
- (42) Bullerjahn, J. T.; Sturm, S.; Kroy, K. Theory of rapid force spectroscopy. *Nat. Commun.* **2014**, *5*, 4463.
- (43) Rognoni, L.; Stigler, J.; Pelz, B.; Ylanne, J.; Rief, M. Dynamic force sensing of filamin revealed in single-molecule experiments. *Proc. Natl. Acad. Sci. U. S. A.* **2012**, *109* (48), 19679–84.
- (44) Austen, K.; Ringer, P.; Mehlich, A.; Chrostek-Grashoff, A.; Kluger, C.; Klingner, C.; Sabass, B.; Zent, R.; Rief, M.; Grashoff, C. Extracellular rigidity sensing by talin isoform-specific mechanical linkages. *Nat. Cell Biol.* **2015**, *17* (12), 1597–606.
- (45) Li, L.; Huang, H. H.; Badilla, C. L.; Fernandez, J. M. Mechanical unfolding intermediates observed by single-molecule force spectroscopy in a fibronectin type III module. *J. Mol. Biol.* **2005**, *345* (4), 817–26.
- (46) Lv, C.; Gao, X.; Li, W.; Xue, B.; Qin, M.; Burtnick, L. D.; Zhou, H.; Cao, Y.; Robinson, R. C.; Wang, W. Single-molecule force spectroscopy reveals force-enhanced binding of calcium ions by gelsolin. *Nat. Commun.* **2014**, *5*, 4623.
- (47) Neumann, J.; Gottschalk, K. E. The integrin-talin complex under force. *Protein Eng., Des. Sel.* **2016**, *29*, 503.